

Strain-mediated electric-field control of resistance in the $\text{La}_{0.85}\text{Sr}_{0.15}\text{MnO}_3/0.7\text{Pb}(\text{Mg}_{1/3}\text{Nb}_{2/3})\text{O}_3-0.3\text{PbTiO}_3$ structure

R. K. Zheng,^{a)} Y. Wang, H. L. W. Chan, and C. L. Choy

Department of Applied Physics and Materials Research Center, The Hong Kong Polytechnic University, Hong Kong, China

H. S. Luo

State Key Laboratory of High Performance Ceramics and Superfine Microstructure, Shanghai Institute of Ceramics, Chinese Academy of Sciences, Shanghai 201800, China

(Received 23 January 2007; accepted 9 March 2007; published online 10 April 2007)

The authors have deposited thin films of $\text{La}_{0.85}\text{Sr}_{0.15}\text{MnO}_3$ (LSMO) on $0.7\text{Pb}(\text{Mg}_{1/3}\text{Nb}_{2/3})\text{O}_3-0.3\text{PbTiO}_3$ (PMN-PT) single-crystal substrates and have achieved modulation of the resistance of the LSMO film by applying an electric field across the PMN-PT substrate whether the LSMO film is in the paramagnetic, ferromagnetic, or charge-ordered state. Piezoelectric measurements show that the electric field gives rise to a lattice strain in the PMN-PT substrate via the converse piezoelectric effect, which then induces a lattice strain and hence a resistance change in the LSMO film. Analysis of the data indicates that the electric-field-induced lattice strain effect dominates over the field effect in the LSMO/PMN-PT structure. © 2007 American Institute of Physics. [DOI: 10.1063/1.2721399]

Mixed valence manganites $\text{La}_{1-x}\text{A}_x\text{MnO}_3$ ($\text{A} = \text{Ca}, \text{Sr}, \text{Ba}$) have attracted considerable attention because of their remarkable physical properties and potential applications.¹⁻⁵ One important question concerning manganite thin films is how the epitaxial strain, which arises from the lattice mismatch between the thin film and the substrate, affects the properties of the thin films. It has been demonstrated that the strain can have drastic effects, such as inducing electronic phase separation,¹ enhancing colossal magnetoresistance effect,² and stabilizing charge-ordered phase.³ Although the strain effect has been investigated extensively, it is almost impossible to isolate the pure strain effect from other extrinsic effects present in real thin-film samples such as structural defects, oxygen nonstoichiometry, chemical inhomogeneities, etc. The effects of strain on the properties of manganite thin films are not yet well understood. In this context, it is desirable to investigate the strain effect using the same thin-film sample so that extrinsic effects can be kept fixed. The $\text{La}_{0.85}\text{Sr}_{0.15}\text{MnO}_3$ (LSMO) compound is an interesting system that exhibits consecutive phase transitions from paramagnetic (PM) state to ferromagnetic (FM) state, and then to charge-ordered (CO) state with decreasing temperature.^{4,5} Thus, LSMO is a good system that can be used for the investigation of the lattice strain effect in the PM, FM, and CO states, respectively.

In this work, we deposited LSMO films on piezoelectric $0.7\text{Pb}(\text{Mg}_{1/3}\text{Nb}_{2/3})\text{O}_3-0.3\text{PbTiO}_3$ (PMN-PT) single-crystal substrates and *in situ* induced lattice strain in the PMN-PT substrate via the converse piezoelectric effect. The responses of the resistance of the LSMO film to the induced lattice strain in the PM, FM, and CO states were studied using the same LSMO/PMN-PT sample.

The PMN-PT single crystals were grown by a modified Bridgman technique.⁶ The single crystals were cut into rectangular plates with dimensions of $10 \times 3 \times 0.55 \text{ mm}^3$ and with the plate normal in the $\langle 001 \rangle$ crystal direction and pol-

ished until the average surface roughness was less than 1 nm. The LSMO films were deposited on the (001)-oriented PMN-PT substrates by dc magnetron sputtering at a substrate temperature of 700 °C.

X-ray diffraction $\theta-2\theta$ scans using a Bruker D8 Discover x-ray diffractometer show that the LSMO films are of single phase and *c*-axis preferentially oriented. Field-emission scanning electron microscopy measurements indicate that the LSMO films have thicknesses of $\sim 35 \text{ nm}$. Low frequency ferroelectric measurements demonstrate that the polarization–electric-field hysteresis loop of the PMN-PT substrate has a square shape and remnant polarization $\sim 25 \mu\text{C}/\text{cm}^2$ and coercive field $E_C \sim 3.3 \text{ kV}/\text{cm}$ [inset (b) of Fig. 1]. The resistance of the LSMO films was measured using the electrical circuit shown in inset (a) of Fig. 1. The leakage current was measured using a Keithley 6517A electrometer and was less than 0.5 nA under a 1 kV/cm bias

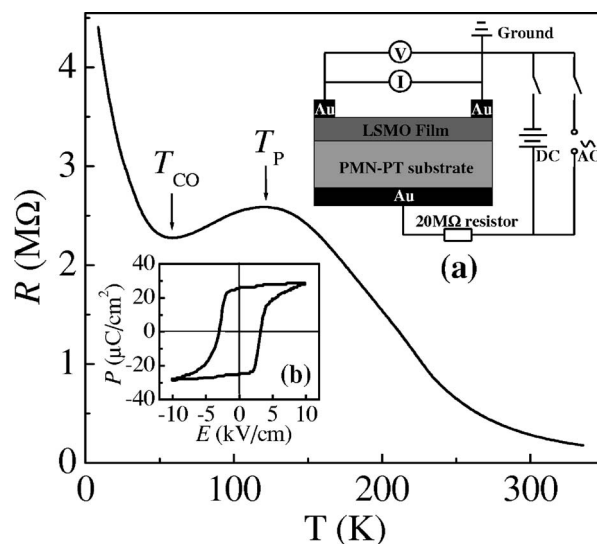


FIG. 1. Temperature dependence of the resistance of the LSMO film. Inset (a) shows the LSMO/PMN-PT structure and the electrical circuit. Inset (b) shows the ferroelectric hysteresis loop of the PMN-PT substrate.

^{a)}Electronic mail: zrk@ustc.edu

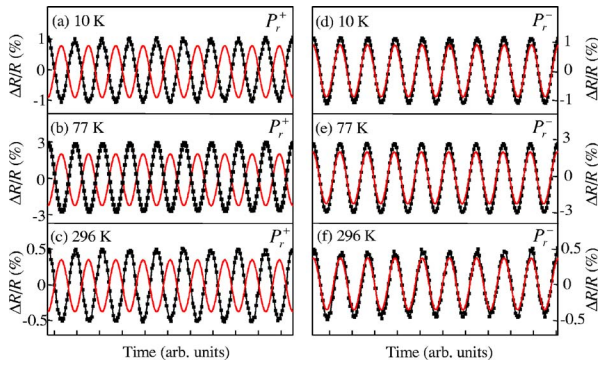


FIG. 2. (Color online) Resistance response of LSMO film at 10, 77, and 296 K as a function of time when a sinusoidal electric field with a peak-to-peak magnitude of 2 kV/cm (full red curves) is applied to the positively (P_r^+) and negatively (P_r^-) polarized PMN-PT substrate, respectively.

field. The electric-field-induced longitudinal lattice displacement of the PMN-PT substrate due to the converse piezoelectric effect was measured using a modified double-beam laser interferometer.

First, we applied a dc poling field of +10 kV/cm across the LSMO/PMN-PT structure which was placed in a silicone oil bath close to the Curie temperature of the PMN-PT substrate so that the PMN-PT substrate was positively polarized (i.e., the electric dipole moments in the PMN-PT substrate point toward the LSMO film; this state is hereafter referred to as P_r^+). Piezoelectric measurements using a Berlincourt-type quasistatic d_{33} meter show that such a positively polarized PMN-PT substrate has a longitudinal piezoelectric coefficient $d_{33} \sim 1350$ pC/N at 296 K.

Figure 1 shows the temperature dependence of the resistance of the LSMO film. In the paramagnetic state the resistance increases with decreasing temperature and reaches a maximum at T_p (~ 122 K), but then it shows a drop with further decrease in the temperature. At a temperature around 58 K the resistance exhibits an upturn, which is associated with the charge ordering.^{4,5,7} These features are similar to those observed in LSMO single crystal.^{4,5} However, the insulator-metal transition temperature T_p and charge-ordering transition temperature T_{CO} are lower than those observed in LSMO single crystal, which could be due to the tensile strain arising from the relatively large lattice mismatch between the LSMO film ($a \sim b \sim c \sim 3.88$ Å) and the PMN-PT substrate ($a \sim b \sim c \sim 4.02$ Å) as well as the oxygen deficiencies.^{8,9}

Figures 2(a)–2(c) show the resistance response ($\Delta R/R$) of the LSMO film as a function of time at 10, 77, and 296 K when a sinusoidal electric field with a peak-to-peak magnitude of 2 kV/cm was applied to the LSMO/PMN-PT structure. The PMN-PT substrate was in the P_r^+ state. Here, $\Delta R/R = [R(E) - R(0)]/R(0)$ where $R(E)$ and $R(0)$ are the resistances of the LSMO film under an electric field E and zero electric field, respectively. It is seen that the resistance of the LSMO film at 10, 77, and 296 K was modulated at the same frequency as that of the driving sinusoidal electric field. The phase difference between the sinusoidal electric field and $\Delta R/R$ is π , which means that applying a positive (negative) electric field to the positively polarized PMN-PT substrate causes a decrease (increase) in the resistance of the LSMO film. The relationship between $\Delta R/R$ and E for PMN-PT in the P_r^+ state can be expressed as $\Delta R/R = -aE$ where a is a positive constant. The peak values of $\Delta R/R$ at 10, 77, and

296 K are about 1.1%, 3.0%, and 0.5%, respectively.

It should be noted that the PMN-PT substrate had been positively polarized before the measurements of the resistance of the LSMO film. Therefore, applying an electric field of 1 kV/cm ($E < E_C$) to the PMN-PT substrate cannot switch the polarization state of the PMN-PT substrate. On the other hand, the electric-field-induced relative change in charge carrier density (Δn) in the LSMO film can be estimated by using the relation $\Delta n/n = \epsilon_0 \epsilon_r V_g / et_i n_0 t_{ch}$,^{10,11} where ϵ_0 and ϵ_r are the permittivities of free space and the PMN-PT substrate, respectively, V_g is the gate voltage, e is the electron charge, t_i and t_{ch} are the thicknesses of the PMN-PT substrate and LSMO film, respectively, and n_0 is the volume density of charge carriers in the LSMO film. Assuming $n_0 \sim 8 \times 10^{21}/\text{cm}^3$ in the LSMO film,¹² $V_g = 55$ V, $t_{ch} \sim 35$ nm, $\epsilon_r = 2550$, and $t_i = 0.55$ mm, one obtains $\Delta n/n = 0.005\%$. In a free electron model, one can obtain the relation $\Delta R/R = -\Delta n/n$.^{13,14} Therefore, the modulation of the resistance of the LSMO film is not due to the field effect in the LSMO/PMN-PT structure since this contribution is negligibly small, compared to the experimentally observed $\Delta R/R$ in the LSMO film.

After the measurements of the resistance of the LSMO film for PMN-PT in the P_r^+ state, the PMN-PT substrate was negatively polarized (referred to as P_r^-) by applying a negative dc poling field (-10 kV/cm) across the LSMO/PMN-PT structure. Figures 2(d)–2(f) show the resistance response ($\Delta R/R$) of the LSMO film as a function of time at 10, 77, and 296 K when a sinusoidal electric field with a peak-to-peak magnitude of 2 kV/cm was applied to the LSMO/PMN-PT structure when the PMN-PT substrate was in the P_r^- state. As seen in Figs. 2(d)–2(f), the resistance of the LSMO film was also modulated by the sinusoidal electric field. However, the resistance change of the LSMO film is in phase with the driving sinusoidal electric field, which is in contrast to those observed in the LSMO/PMN-PT structure for P_r^+ [Figs. 2(a)–2(c)]. The peak values of $\Delta R/R$ at 10, 77, and 296 K are about the same as those observed in the LSMO/PMN-PT structure for PMN-PT in the P_r^+ state.

PMN-PT is a ferroelectric material and thus exhibits the converse piezoelectric effect after it has been either positively or negatively polarized. When an electric field E ($E < E_C$) is applied to the polarized PMN-PT substrate, the lattice of the PMN-PT substrate will expand (or contract) along the direction of the electric field.¹⁵ Figures 3(a) and 3(b) show the electric-field-induced longitudinal lattice displacement (Δl) of the PMN-PT substrate when a sinusoidal electric voltage with a peak-to-peak magnitude of 20 V is applied to the positively and negatively polarized PMN-PT substrate, respectively. Here, $\Delta l = l(E) - l(0)$ where $l(E)$ and $l(0)$ are the thicknesses of the PMN-PT substrate under an electric field E and zero electric field, respectively. It can be seen that the electric field causes the lattice of the PMN-PT substrate to expand and contract along the c axis at the same frequency as that of the field. When a positive (negative) voltage of 10 V is applied to the positively polarized PMN-PT substrate, the lattice of the PMN-PT substrate expands (contracts) along the c axis by ~ 13.6 nm. In contrast, when a positive (negative) voltage of 10 V is applied to the negatively polarized PMN-PT substrate, the lattice of the PMN-PT substrate contracts (expands) along the c axis by ~ 13.6 nm [Fig. 3(b)]. The electric-field-induced lattice dis-

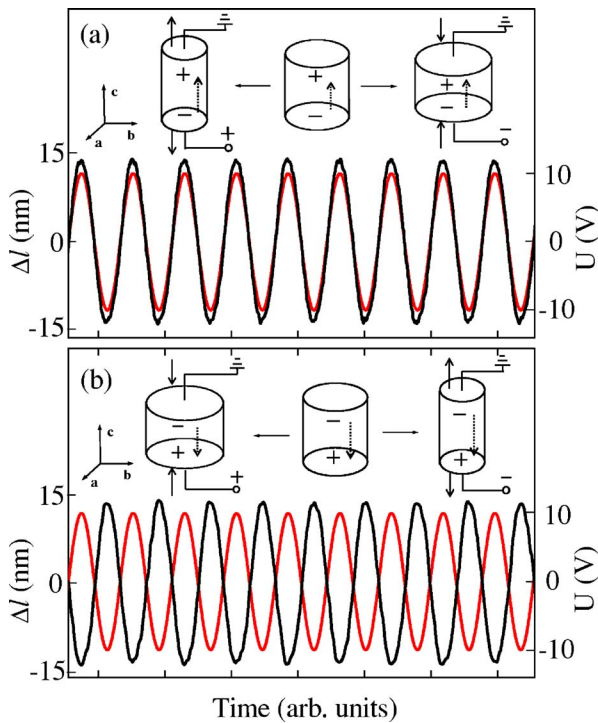


FIG. 3. (Color online) Electric-field-induced longitudinal lattice displacement (Δl) of the PMN-PT substrate at 296 K as a function of time when a sinusoidal electric voltage with a peak-to-peak magnitude of 20 V (full red curves) is applied to the positively (a) and negatively (b) polarized PMN-PT substrate, respectively. The insets in (a) and (b) are schematic diagrams showing the electric-field-induced expansion and contraction of the lattice of the PMN-PT substrate via the converse piezoelectric effect. The dotted arrows represent the direction of polarization.

placements (Δl) in ferroelectric materials due to the converse piezoelectric effect can be calculated using the relation $\Delta l = d_{33}V$.¹⁵ Setting $d_{33} = 1350$ pm/V and $V = 10$ V, one obtains $\Delta l = 13.5$ nm. This calculated value agrees well with the Δl value obtained from displacement measurements, strongly indicating the piezoelectric nature of the strain.

The modulation of resistance can be understood in terms of the converse piezoelectric effect. When a positive (negative) electric field is applied to the positively polarized PMN-PT substrate, the out-of-plane lattice parameter of the PMN-PT substrate increases (decreases) while the in-plane lattice parameters decrease (increase) [insets of Fig. 3(a)]. Such a change in the lattice parameters of the PMN-PT substrate will lead to a decrease (increase) in the magnitude of the tensile strain in the LSMO film, thereby causing a decrease (increase) in the resistance of the LSMO film.¹⁶ As a result, the resistance of the LSMO film is modulated with the same frequency (but the opposite phase) as those of the driving sinusoidal electric field. In contrast, when a positive (negative) electric field is applied to the negatively polarized PMN-PT substrate, the out-of-plane lattice parameter of the PMN-PT substrate decreases (increases) while the in-plane lattice parameters increase (decrease) [insets of Fig. 3(b)], which will lead to an increase (decrease) in the magnitude of the tensile strain in the LSMO film, thereby causing an increase (decrease) in the resistance of the LSMO film.¹⁶ Consequently, the resistance of the LSMO film is modulated with the same frequency and phase as those of the driving sinusoidal electric field.

The electric-field-induced in-plane strain (ε_{\parallel}) in the PMN-PT substrate can be calculated using the relation $\varepsilon_{\parallel} =$

$-d_{31}E$ where d_{31} is the transverse piezoelectric coefficient of the PMN-PT substrate.¹⁵ Using $d_{31} = 620$ pC/N obtained by a resonance technique using an HP4294A impedance analyzer, one obtains $\varepsilon_{\parallel} = -0.0062\%$ when an electric field of 1 kV/cm is applied to the polarized PMN-PT substrate. Thus, the absolute value of the resistance-strain coefficient $(\Delta R/R)/\varepsilon_{\parallel}$ for P_r^+ and P_r^- at 296 K ~ 81 , respectively. It should be noted that a value of $(\Delta R/R)/\varepsilon_{\parallel} \sim 150$ was observed previously in a $\text{La}_{0.7}\text{Sr}_{0.3}\text{MnO}_3/0.72\text{Pb}(\text{Mg}_{1/3}\text{Nb}_{2/3})\text{O}_3-0.28\text{PbTiO}_3$ structure at 300 K.¹⁶

In summary, we have reported the possibility of electric-field control of resistance of LSMO films grown on piezoelectric PMN-PT substrates. The resistance of the LSMO film in the PM, FM, and CO states can be modulated by applying a sinusoidal electric field across the PMN-PT substrate. The modulation of the resistance arises from the induced lattice strain in the LSMO film, which is induced by the lattice strain in the PMN-PT substrate resulting from the converse piezoelectric effect. The induced lattice strain in the PMN-PT substrate may increase or decrease the magnitude of the tensile strain in the LSMO film, which depends on both the polarization state of the PMN-PT substrate and the polarity of the electric field applied to the PMN-PT substrate. The experimental results also show that a decrease (increase) in the tensile strain in the LSMO film reduces (enhances) the resistance of the LSMO film whether the LSMO film is in the PM, FM, or CO state.

This work was supported by the Postdoctoral Fellowship Scheme (Program No. G-YX40) and the Centre for Smart Materials of The Hong Kong Polytechnic University.

¹A. Biswas, M. Rajeswari, R. C. Srivastava, T. Venkatesan, R. L. Greene, Q. Lu, A. L. de Lozanne, and A. J. Millis, *Phys. Rev. B* **63**, 184424 (2001).

²H. S. Wang and Q. Li, *Appl. Phys. Lett.* **73**, 2360 (1998).

³W. Prellier, Ch. Simon, A. M. Haghiri-Gosnet, B. Mercey, and B. Raveau, *Phys. Rev. B* **62**, R16337 (2000).

⁴Y. Yamada, O. Hino, S. Nohdo, R. Kanao, T. Inami, and S. Katano, *Phys. Rev. Lett.* **77**, 904 (1996).

⁵G. T. Woods, P. Poddar, H. Srikanth, and Y. M. Mukovskii, *J. Appl. Phys.* **97**, 10C104 (2005).

⁶H. S. Luo, G. S. Xu, H. Q. Xu, P. C. Wang, and Z. W. Yin, *Jpn. J. Appl. Phys., Part 1* **39**, 5581 (2000).

⁷R. Klingeler, J. Geck, R. Gross, L. Pinsard-Gaudart, A. Revcolevschi, S. Uhlenbruck, and B. Büchner, *Phys. Rev. B* **65**, 174404 (2002).

⁸M. Itoh, K. Nishi, J. D. Yu, and Y. Inaguma, *Phys. Rev. B* **55**, 14408 (1997).

⁹A. M. D. Léon-Guevara, P. Berthet, J. Berthon, F. Millot, A. Revcolevschi, A. Anane, C. Dupas, K. L. Dang, J. P. Renard, and P. Veillet, *Phys. Rev. B* **56**, 6031 (1997).

¹⁰K. Nakajima, K. Yokota, H. Myoren, J. Chen, and T. Yamashita, *Appl. Phys. Lett.* **63**, 684 (1998).

¹¹D. W. Greve, *Field Effect Devices and Applications: Devices for Portable Low-Power, and Imaging Systems* (Prentice-Hall, Englewood Cliffs, NJ, 1998), Chap. 2, p. 18.

¹²Y. Lyanda-Geller, S. H. Chun, M. B. Salamon, P. M. Goldbart, P. D. Han, Y. Tomioka, A. Asamitsu, and Y. Tokura, *Phys. Rev. B* **63**, 184426 (2001).

¹³X. X. Xi, C. Doughty, A. Walkenhorst, C. Kwon, Q. Li, and T. Venkatesan, *Phys. Rev. Lett.* **68**, 1240 (1992).

¹⁴T. Kanki, Y. G. Park, H. Tanaka, and T. Kawai, *Appl. Phys. Lett.* **83**, 4860 (2003).

¹⁵B. Jaffe, W. R. Cook, Jr., and H. Jaffe, *Piezoelectric Ceramics* (Academic, New York, 1971), Chap. 2, p. 8.

¹⁶C. Thiele, K. Dörr, S. Fähler, L. Schultz, D. C. Meyer, A. A. Levin, and P. Paufler, *Appl. Phys. Lett.* **87**, 262502 (2005).

Applied Physics Letters is copyrighted by the American Institute of Physics (AIP). Redistribution of journal material is subject to the AIP online journal license and/or AIP copyright. For more information, see <http://ojps.aip.org/aplo/aplcr.jsp>